Version of Record: https://www.sciencedirect.com/science/article/pii/S030645491930489X
Manuscript_087835469ebedf7172b323936308c319

Passive Decay Heat Removal System Design for the Integral Inherent Safety Light Water Reactor (I^2S-LWR)

Mingjun Wang[1,2], Annalisa Manera*[2], Victor Petrov[2], Matthew J. Memmott[3], Suizheng Qiu*[1], G. H. Su[1]

(1. Department of Nuclear Science and Technology, Xi'an Jiaotong University, Xi'an 710049, China;

2. Department of Nuclear Engineering and Radiological Sciences, University of Michigan, Ann Arbor, MI 48109, USA

3. Brigham Young University, 350 Clyde Building, Provo UT, 84602, USA)

Email: manera@umich.edu; szqiu@mail.xjtu.edu.cn

Abstract: The Integral, Inherently Safe Light Water Reactor (I^2S-LWR) is an innovative Pressurized Water Reactor (PWR) concept being developed by a multi-institutional team led by Georgia Tech and in collaboration with Westinghouse, under the Department of Energy's Nuclear Energy University Programs Integrated Research Projects (DOE NEUP IRP). The University of Michigan leads the design of the thermal-hydraulic and passive safety systems, in collaboration with Westinghouse and Bringham Young University. The I^2S-LWR features an integral primary system configuration and is more conducive to the implementation of inherent safety features by eliminating potential accidents. In this paper, a novel passive Decay Heat Removal System (DHRS), is presented, consisting of a primary loop, an intermediate loop and a cooling tower loop. This passive system is designed to remove the I^2S-LWR decay heat in the case of emergency heat removal transients, without the need for external power or operator action. The proposed DHR uses atmosphere as ultimate heat sink, to achieve indefinite decay heat removal. In this paper, firstly, the design of primary and secondary DHRS heat exchangers is optimized. Then the DHR heat removal characteristics are studied using the best-estimate thermal hydraulic code RELAP5. In addition, CFD simulations have been performed in order to investigate the DRHS helical coil primary heat exchanger performance with different coil pipe arrangements, and optimize its design. The performance of the proposed DHRS concept is investigated in case of a Station Black-Out (SBO) scenario. Operation of two, three and four DHRS trains is studied respectively. The results show that three out of four DHRS trains are sufficient to indefinitely remove the core decay heat successfully during a SBO, and keep the reactor in a safe state without the need of any other auxiliary active system.

Keywords: DHR, Integral reactor, Station Black-Out, Heat removal

1. Introduction

The I^2S-LWR [1] is a novel reactor concept being developed by a multi-institutional team, under the Department of Energy's Nuclear Energy University Programs (NEUP) Integrated Research Projects (IRP), aiming to implement inherent safety features by eliminating potential accident initiators and by using novel passive safety systems. The I^2S-LWR builds on other integral reactor designs, such as the International Reactor Innovative and Secure (IRIS) [2] and the Westinghouse Small Modular Reactor (W-SMR) [3], and it incorporates novel features to allow for much higher power outputs (in the range of 1000 MWe) while still maintaining an integral configuration.

Several significant innovative design concepts are applied to the I^2S-LWR. The passive safety systems of the I^2S-LWR are designed to achieve long-term (indefinite) decay heat removal using ambient air as ultimate heat sink, without the need for either an external power supply or replenishment of coolant supply. Moreover, a novel approach to instrumentation and monitoring will ensure that plant status is reliably known in normal, off-normal, and especially post-accident conditions. Finally, the whole nuclear island will be seismically isolated to guarantee its protection against earthquakes with magnitude within the historical record, and to limit the consequences of stronger earthquakes. The enabling innovation is the use of high power density technologies/components in synergy with an integral configuration. A compact core design is achieved by using a non-oxide fuel form with improved heat removal capability, combined with fuel/clad design of enhanced accident tolerance. This allows increasing core power density while at the same time improving the core safety performance and response in transient/accident scenarios. The novel steam generating system is based on very compact primary Printed Circuit micro-channel Heat eXchanger (PCHX) in combination with flashing drums [4], which makes a 1,000 MWe power level compatible with an integral configuration.

In addition to the systems and components contained in the Reactor Pressure Vessel (RPV) of typical, non-integral designs, the I^2S-LWR pressure vessel includes Control Rod Drive Mechanisms (CRDM), the pressurizer, the primary HXs and the Decay Heat Removal System (DHRS) HXs. Fig. 1 shows the I^2S-LWR RPV and the internals layout.

Passive Safety is a fundamental concept proposed for new generation Nuclear Power Plant (NPP) designs. The basic idea is to remove heat from the reactor core by relying on natural circulation, gravity, or other physical mechanisms that do not require an external power source. The employment of passive safety systems has been proved to improve the NPP safety level in case of emergency conditions and reduce considerably the Core Damage Frequency (CDF). Early studies concluded that passive safety systems are technically and

economically applicable to small and midsize NPPs, and that they can be applied to both Boiling Water Reactor (BWR) and Pressurized Water Reactor (PWR) technologies [6]. In recent years, research has been focused on the application of passive safety systems in large power LWRs [7-9]. Plant designs like AP1000 (Westinghouse) [10], KERENA (former SWR1000, AREVA), ESBWR (GE) and V-392 (Gidropress) [11] have adopted an extensive use of passive systems to improve the NPP safety, relying on gravity, compressed gas, natural circulation, and evaporation for long term reactor cooling in accidental events. A station blackout accident simulation for a typical PWR where high and medium pressure injection pumps were replaced by passive injection components was performed using RELAP5 code, in order to analyze the degree of plant safety (without any operator action) by using only the passive components [12]. It demonstrates that the reactor safety level could be improved by passive safety system. Research on heat removal by in-pool immersed heat exchangers (HXs) was performed at SIET laboratories using the PERSEO facility by experimental method [13].

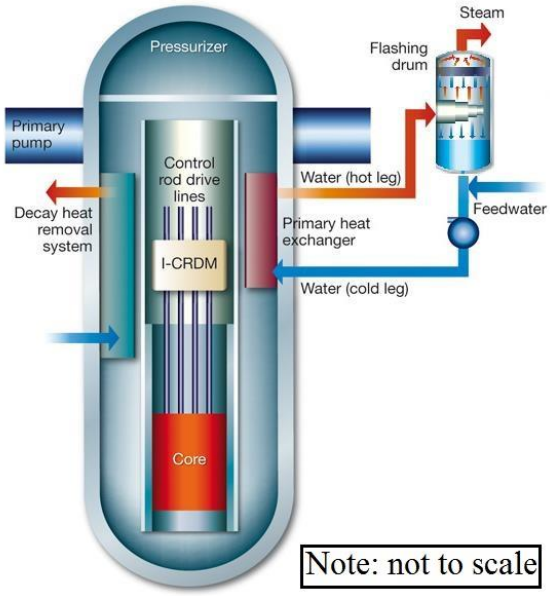

Fig. 1 I^2S-LWR configuration [5]

Learning from past experience, with the I^2S-LWR design it is proposed to further increase LWRs safety beyond that of Gen-III+ and toward inherent safety by:

- Eliminating accident initiators as far as achievable: in the I^2S-LWR, large and intermediate break LOCAs are eliminated by design. The only potential LOCA scenarios include SBLOCA as a consequence of a stuck-open PORV, and the break of a Control Volume System (CVS) pipeline. There may also be the potential for small (≤ 1") breaks of service lines (such as cooling of pump motors if seal-less pumps with external HXs are used, etc);

- Limiting the loss of inventory during LOCA scenarios: the I^2S-LWR design feature a compact pressurized containment. Loss of inventory is limited by a set of systems which allow to quickly reach pressure equilibrium between RPV and containment, similar design concept with the IRIS design [2];
- Increasing the level of passivity of all foreseen safety systems to the IAEA passivity level C [14] and above, limiting the use of components which require moving parts.

By eliminating both intermediate and large-break LOCAs scenarios, by limiting the loss of inventory during SBLOCAs, by foreseeing passive safety features which do not rely on stored energy (batteries, etc.), and by using atmosphere as the ultimate heat sink, a long-term (theoretically indefinite) self-sustained decay heat removal capability can be achieved, with no need for intervention in case of an accident with loss of external power.

The safety philosophy of the I^2S-LWR design is based on three consecutive lines of defense:

- The first and main line of defense is aimed at preventing core damage, especially in the event of a prolonged loss of offsite power. This is pursued by eliminating event precursors as far as achievable, by limiting the loss of RPV inventory in case of LOCAs, and by designing safety systems with a very high degree of passivity;
- The second line of defense is aimed at cooling the containment vessel by air or other medium in natural circulation regime;
- The third line of defense is aimed at protecting the Containment Vessel (CV) from external events. This is accomplished by partially burying the CV, so that the risk of a plane crash can be reduced, and by placing the CV on seismic isolators to mitigate the effect of earthquakes. The safety systems are designed with level of passivity C, so that even in the event of a flood the reactor will not suffer any damage.

The passive safety systems foreseen for the containment cooling are illustrated in a companion paper and in Ref. [15], where their performance is demonstrated against an inadvertent opening of PORV (Power Operated Relief Valve) accident. The present paper is instead focused on the design of the DHRS, aimed at removing the decay heat from the primary loop, using external atmosphere as the ultimate heat sink.

The DHRS proposed in the present paper for the I^2S-LWR design consists of four independent trains. Each train includes a helical coil HX located in the RPV, an intermediate loop and a dry cooling tower system. The DHRS is designed to remove the reactor core decay heat in case of loss of the secondary side heat sink, maintaining the reactor in a safe state.

In the following section, the detailed design of the DHRS is presented. A RELAP5 model of the I^{2}S-LWR primary loop and DHRS is then employed to investigate the DHRS heat removal characteristics in the event of a Station Black-Out (SBO).

2. DHRS Design for the I^{2}S-LWR

The passive DHR is the main safety related system foreseen for the I^{2}S-LWR [16] to bring the reactor to a safe-shut-down state without the need for an external power source and/or operator action. In the design we propose, the DHRS is comprised of four trains, each consisting of a primary HX located in the RPV, a secondary HX located in a dry cooling tower, a fail-open valve, and the required piping between these components. A single train is illustrated in Figure 2. There are two thermally coupled loops (hydraulically isolated) that are used to transfer heat from the reactor to the environment. The helical coil design is chosen for the primary HX because it provides high heat transfer capability in a limited space, while maintaining low pressure drops, important to guarantee a sufficient degree of natural circulation. Both inlet and outlet legs of the helical coils are placed in the downcomer, the outlet leg being located at an elevation close to the core inlet, and the inlet leg placed just below the elevation of the core outlet. An intermediate loop, operated with pressurized water (7.0 MPa), is used to transfer heat from the primary HX to a dry cooling tower, where atmosphere is used as the ultimate heat sink.

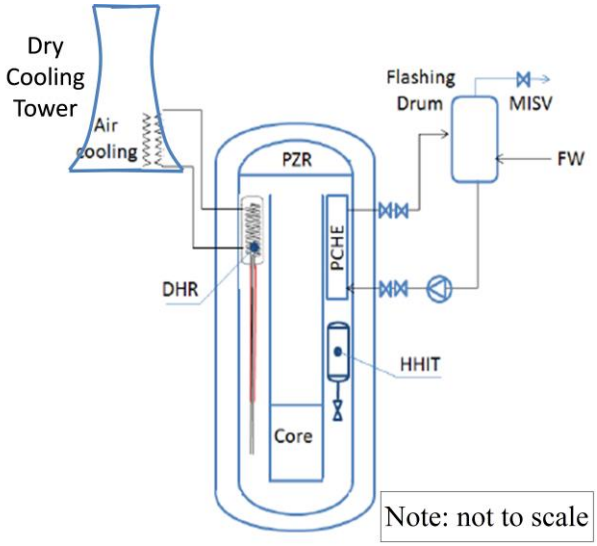

Fig. 2 Illustration of DHRS Concept, Including Arrangement in Reactor Vessel

As alternative designs we have considered:

- Inlet leg of the primary DHR helical coil HX placed at the exit of the core. While this would allow for higher natural circulation in the DHR because of the higher temperature gradient between inlet and outlet legs of the HX, it also involves additional design challenges as the DHR inlet leg would have to

be accommodated in the RPV upper plenum where control rod drive mechanisms and other internals are present;

- Molten salt or nanofluids as operating fluid for the intermediate DHR loop. Molten salts would enable natural circulation without employing long vertical pipe sections, which are otherwise needed when water is used instead. Molten salt however adds the challenge of salt solidification, which needs to be prevented at all times. The use of water with nanofluids has the advantage of enhanced heat transfer. Long vertical pipe sections of the intermediate loop including loop pressurization would be needed in this case, as for the base design.

Currently, the above alternatives have not been included in the final design, as our preliminary analyses reported in the next chapter have shown that the base DHRS design performs adequately.

2.1 Helical Coil HX Design

The primary DHRS HX consists of a helical coil design optimized for natural circulation flow. These exchangers were pioneered with the Otto Hahn reactor, and are known for their low hydraulic resistances, high surface area, and low mechanical and thermal stresses [17, 18]. They are currently proposed by NuScale for their natural circulation reactor [19]. The helical tubes are held in place by vertical baffles with alternating holes [20], as illustrated in Figure 3. In our present design, each coil within this annular region contains a number of tubes dictated by the coil radius and the axial tube pitch. The number of coils that fit within the annular region is dictated by the radial tube pitch and tubes diameter. Each coil also winds around the inner flow pipe in the opposite direction as the immediately adjacent coils, either clockwise or counter-clockwise. A MATLAB script is used to optimize all the helical coil HX parameters [16].

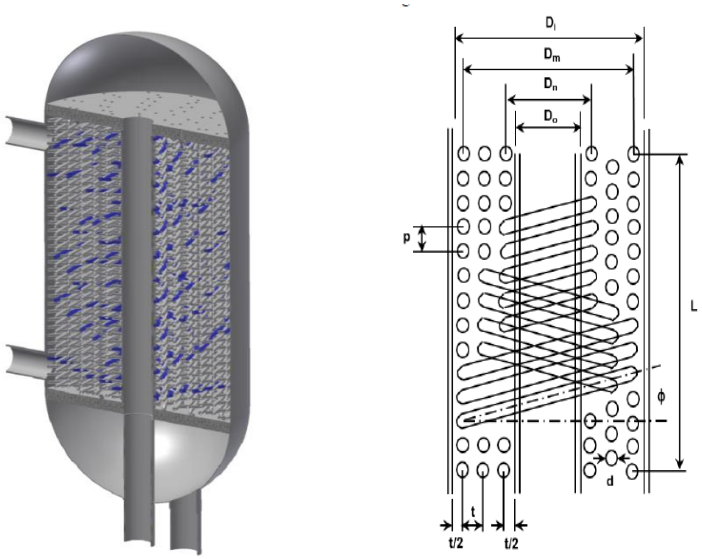

Fig. 3 DHRs primary helical coil HX configuration

The base design specifications of the helical coil exchanger can be found in Table 1. These initial parameters were then optimized through a series of parametric studies of each major parameter of the DHRS primary helical coil exchanger.

Table 1 Main base parameters of helical coil HX

Parameters	Meaning	Designed value
L	Height of HX	8.0m
D_i	Outer shell inner wall diameter	0.7 m
D_o	Inner shell outer wall diameter	0.11 m
d_o	Tube outer diameter	0.013 m
d_i	Tube inner diameter	0.0111 m
P	Axial pitch	0.0286 m
D_{downc}	Down-comer primary side DHR	0.0737 m
N_{coils}	Number of coils	9
T	Radial pitch	0.0344 m
Φ	Average inclination angle	-12.4 °

2.2 Cooling Tower Design

The second DHR exchanger is a water-air exchanger located within a dry cooling tower, and is used to transfer heat from the intermediate loop to air in the environment. The general cooling tower shape is a hyperboloid. The hyperboloidal shape allows for a better air flow distribution and helps reducing the wind impact on the structure [21]. Generally, the shape of a hyperboloidal cooling tower shell consists of a lower and an upper hyperbola branch, which both meet at the throat (see Figure 4). The hyperbola axis does not need to correspond with the tower axis. Thus the curvature of the meridian varies over the tower height, in general with a maximum at the throat [22].

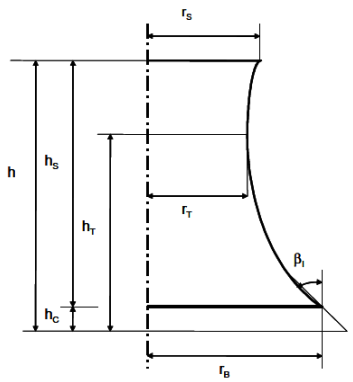

Fig. 4 Cooling tower geometric diagram [23]

The HX tube arrangement is another important factor that needs to be considered carefully. In most practical towers the HX bundles are arranged either vertically around the circumference of the tower or horizontally at the inlet cross section (see Figure 5). There are two possible arrangements for the horizontal configuration: rectangular and radial (see Figure 5.b and 5.c respectively). For each of these, only a part of the available cross section is occupied with HX tubes.

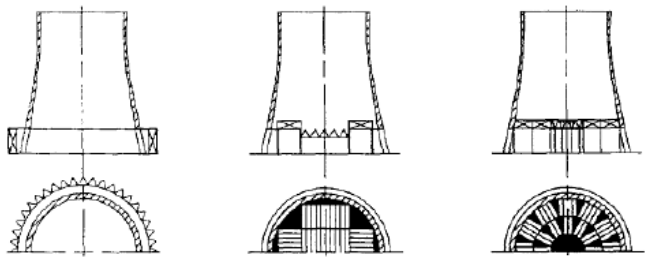

(a) (b) (c)

Fig. 5 HX bundles arrangements: (a) Vertical circumferential; (b) Horizontal rectangular; (c) Horizontal radial [23]

Based on the results on full scale measurements, Moore [23] concluded that the heat transfer performance of the internal horizontal arrangement is less susceptible to wind variations than the vertical configuration. In windless condition the heat rejection rate of a cooling tower is instead independent of the particular tube arrangement, for a given total HX surface area.

The total tower height h, column height h_C and base shell radius r_B are generally fixed by the thermal design, likewise the throat radius r_T, with small admissible variability. The shell radius r_S must be not smaller than r_T to avoid flow perturbation. All other parameters can be freely selected within certain design limits. However, the geometrical parameters are in typical proportions between them [24], in order to optimize construction and esthetics of the cooling tower. The angle β of the shell inclination is restricted by:

$$\tan \beta_I \geq (r_B - r_T) / (h_T - h_C) \quad (1)$$

The other parameter constraints are shown in the following equations [25]:

$$\frac{(2 \times r_B)}{h} = 0.75 \quad (2)$$

$$\frac{r_T}{r_B} = 0.55 \quad (3)$$

$$\frac{h_C}{(2 \times r_B)} = 0.75 \quad (4)$$

$$r_s = r_T \quad (5)$$

$$L = r_B/\sqrt{5} \quad (6)$$

All the main parameters of the cooling tower are reported in Table 2. The sign of equality herein designates the smallest possible value of β_I, at which limit condition two conical frusta meet at the throat in a break point of infinite curvature. The maximum angle β_I is limited by the maximum possible inclination of the form-work system for the shell construction, by experience noticeable below 20°. It is an interesting fact that most of the above mentioned technical aspects improve for larger β_I, except for the aesthetics of the structure: a cooling tower generally is perceived as more pleasant for medium values of β_I.

Table 2 Main parameters of cooling tower

Parameters	Meaning	Designed value
H	Total tower height	20 – 40 m
r_e	Tube radius	0.0125 m
r_B	Base shell radius	11.25 m
r_T	Tower throat radius	6.19 m
h_c	Base shell height	2.25 m
h_t	Tower throat height	26.07 m
r_S	Superior shell radius	6.19 m
N_r	Axial tubes raw number in the HX per each train	96
N_{total}	Total tubes number in the HX per each train	38592

2.3 DHR System Optimization and Heat Removal Characteristic Study

There are two primary challenges to the utilization of this particular passive DHRS: the first is ensuring sufficient heat transfer in the air/water HX. The second is ensuring that natural circulation flow is sufficient to remove decay heat prior to a significant buildup of energy within the RPV.

The performance of the DHRS helical coil loop and dry cooling tower is investigated in this section using the RELAP5 best-estimate thermal-hydraulic code [26-28]. A RELAP5 model of the DHRS, shown in Figure 6, was developed in order to finalize the optimization of the system dimensions. The design envelope for the various components within the DHR was determined by means of sensitivity studies, reported in section 2.3.1. The relevant DHRS operational parameters used for the study are listed in Table 3.

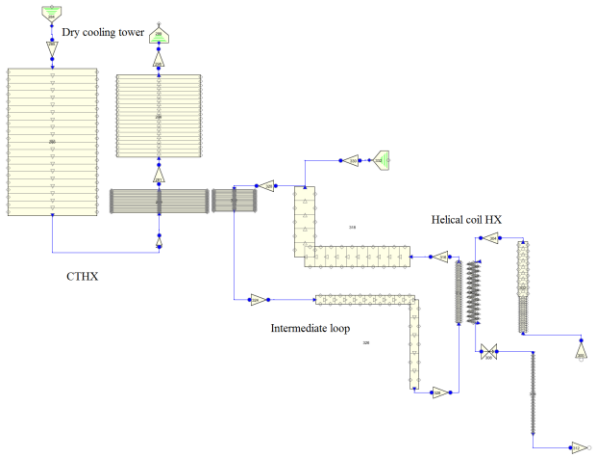

Fig. 6 RELAP5 nodalization for DHRS optimization studies

Table 3 DHRs Operational Parameters

DHRS operation parameters	Value
Primary Inlet Temperature (K)	597.04
Primary Outlet Temperature (K)	576.21
Water Inlet Pressure (MPa)	15.51
Intermediate Loop Temperature (K)	322.04
Intermediate Loop Pressure (MPa)	6.89
Cooling Tower Air Temperature (K)	283.15 - 323.15
Cooling Tower Air Pressure (MPa)	0.1

2.3.1 Helical coil HX sensitivity study

On the basis of geometrical consideration and starting from the base design summarized in Table 1, an optimization routine containing all relevant geometrical constraints (see scheme in Figure 7) has been written in MATLAB. Starting with the DHRS primary HX shell height, shell diameter, helicoidal tubes diameter and tubes axial pitch, the MATLAB routine optimizes radial pitch, number of tubes, inclination angle of coils and tube length in order to maximize the heat transfer surface. This methodology significantly reduces the number of RELAP5 simulations necessary to complete the optimization procedure.

In order to perform parametric studies on the DHRS primary side (PEHX), the RELAP5 nodalization shown in Figure 6 was modified to maximize heat removal from the PEHX shell side (component 324 in Figure 6). In this way the resulting maximum heat removal is dictated by the DHRS primary side only. The results of the RELAP5 sensitivities are reported in Figure 8 to Figure 10. The variables selected for the optimization are the DHRS coil diameters, the radial pitch between coils, the DHRS height and the DHRS diameter. Because of the

optimization already performed by means of the MATLAB script, there is little variability of the heat transfer power in the second optimization performed with RELAP5.

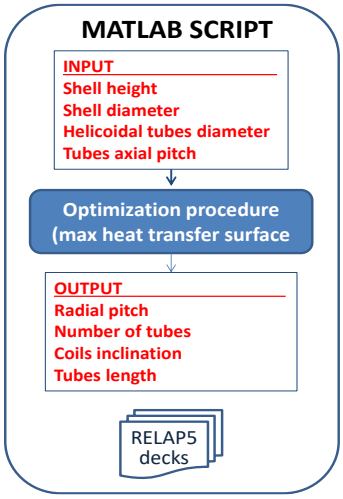

Fig. 7 Optimization procedure for DHRS helicoidal HX dimensioning

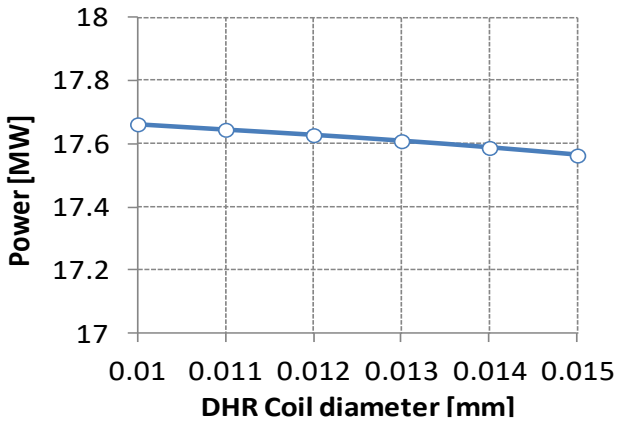

Fig. 8 Decay heat removal as a function of DHR coil diameter

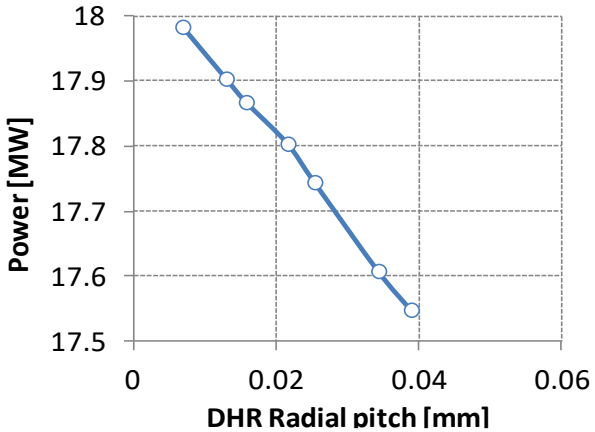

Fig. 9 Decay heat removal as a function of DHR radial pitch

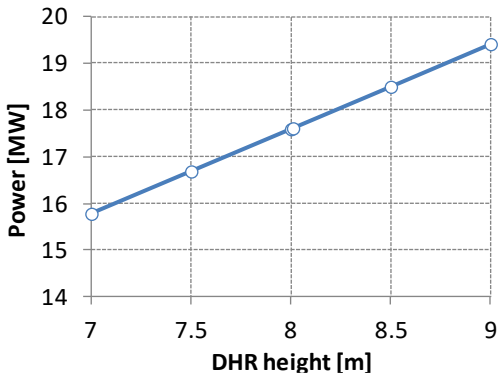

Fig. 10 Decay heat removal as a function of DHR height

The parameter that is mostly affecting the performance of the DHRS primary side is the DHRS shell height. This is limited, however, by the overall RPV height. The initial height of 8.0 m allows a heat removal capability of about 17.5 MW per DHRS train, which seems to be appropriate at this stage of the I^2S-LWR design. Transient simulations of the DHRS performance during accident conditions are necessary to determine whether the current DHRS design needs further modifications.

2.3.2 Helical coil HX study using Computational Fluid Dynamics (CFD)

(1) Geometry

Because of the geometrical complexity of the helical coils HX design, the impact of multi-dimensional effects has to be considered on local heat transfer and flow characteristics CFD analyses have been performed for two different pipe patterns, a chess and a uniform configuration respectively, due to the coils alternation along the main flow direction, as illustrated in Figure 11.

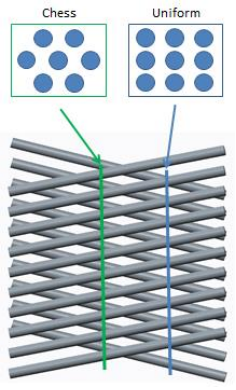

Fig. 11 Two helical coil HX views

The CFD models for the two configurations are presented in Figure 12. In the figure, flow direction, axial pitch and radial pitch are also indicated. 25 axial rows of coils are considered.

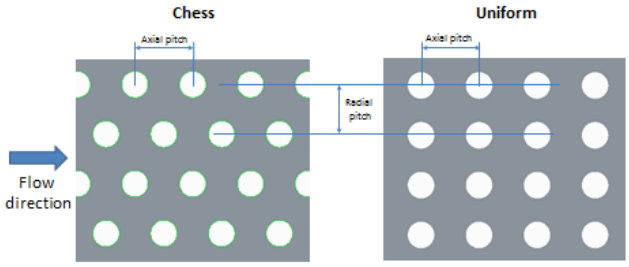

Fig. 12 The helical coil HX 2-D view

Fixing the HX shell dimensions, CFD simulations have been performed for three different radial pitches, leading to 8 coils, 9 coils and 10 coils respectively. The distance between the side tube and the HX shell wall was varied between Pitch/2 and Pitch/4 are chosen to study the influence of different tube arrangements on the HX performance. Figure 13 illustrates all the six different type arrangements.

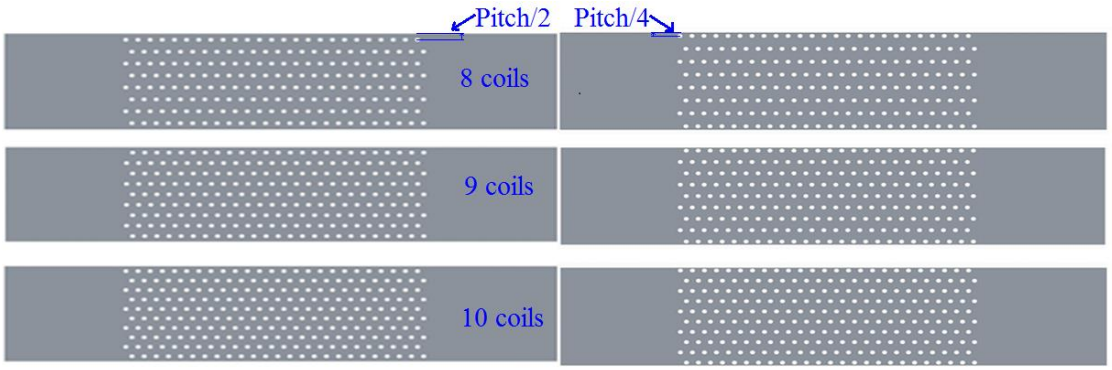

(a) (b)

Fig.13 Two types coil arrangements (a) Side tubes close to the wall (~Pitch/2); (b) Side tubes close to the wall (~Pitch/4)

The boundary conditions applied to the model are shown in Fig. 14. The tube heat flux is set to 67532.0 W/m^2 and the inlet mass flow rate to 0.163 kg/s. Symmetry boundary conditions are applied to the upper and lower part of the model, and the remaining surfaces are set as wall boundary conditions.

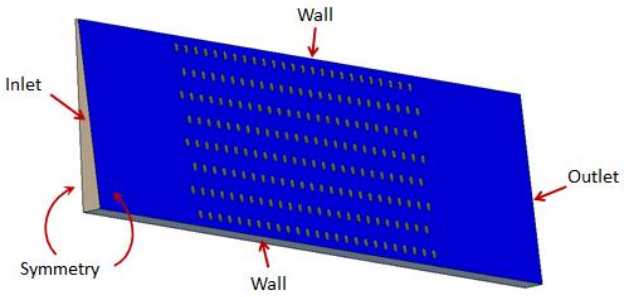

Fig. 14 Model boundary

(2) Meshing

A hexahedral mesh type has been used for the CFD simulations, as shown in Fig. 15, including mesh refinement in the proximity of the walls.

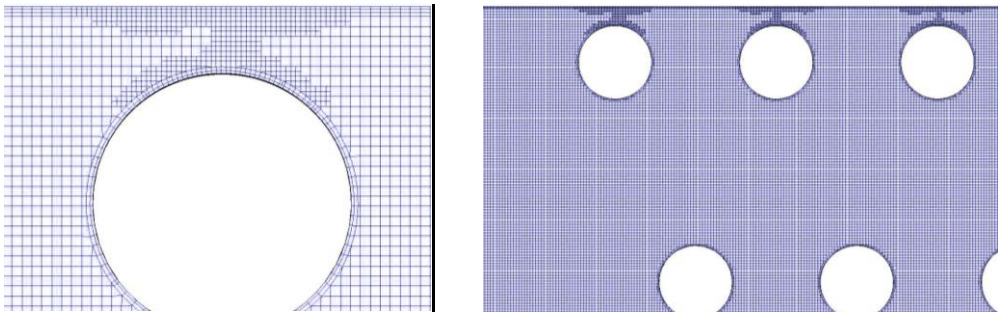

Fig. 15 Computational CFD mesh

A mesh sensitivity study has been performed using three mesh sizes, as presented in Fig. 16. Coarser meshes with cell base size larger than 1mm were not considered because such meshes would present too few cells between successive coils in the case of tight pitch. Selected cell base sizes for the mesh sensitivity study are 1.0 mm, 0.5 mm and 0.25 mm, respectively, leading to 370000, 1400000 and 5440000 cells in this study. Additional convergence studies have been carried out to ensure adequate mesh refinement in the proximity of the walls. The CFD simulations have been performed using the commercial code STARCCM+.

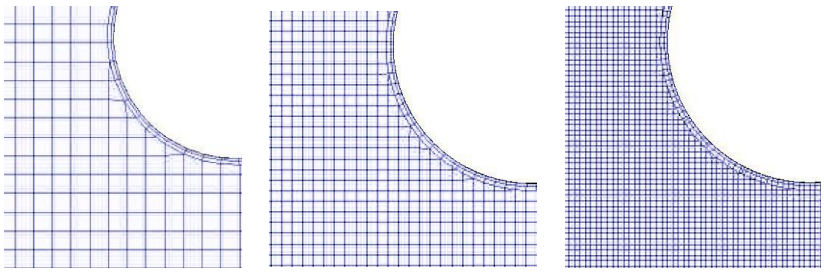

Mesh 1 mesh 2 Mesh 3

Fig 16 Three different mesh sizes

Figs. 17 shows the variation of pressure drop between inlet and outlet (delta P) of the computational domain as function of the mesh size. Good convergence is obtained, with maximum pressure drop variation on different meshes of about 3.6%. In order to balance accuracy and computational requirements, mesh 1 was selected for our investigations. In addition, three integration time steps were evaluated for each mesh (0.1s, 0.01s, and 0.001s respectively). The result shown in Fig.18 illustrates that an integration time step of 0.01 s is suitable for our purposes.

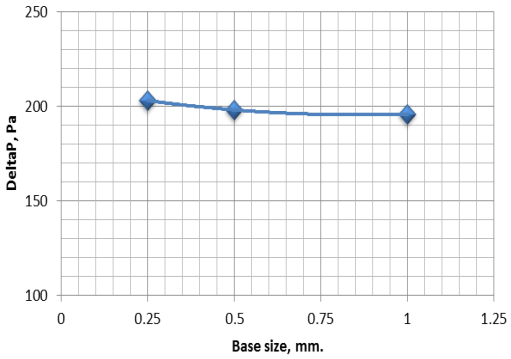

Fig. 17 Variation of Delta P with base size

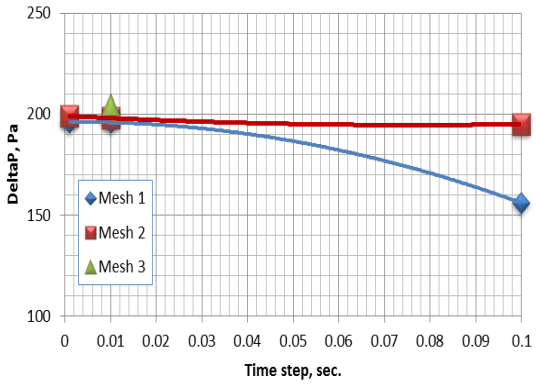

Fig. 18 Variation of Delta P with time step for three mesh sizes

(3) Calculation results

The Heat Transfer Coefficient (HTC), pressure drop and temperature difference between inlet and outlet are estimated as function of the number of coils using STARCCM+. An additional variable for the HX design is the distance between the side tube and the shell wall. Simulations were performed for two different distances, equal to pitch/4 and pitch/2 respectively, with the pitch being the radial distance between the centers of two consecutive tubes.

The results for Delta P, Delta T, and HTC are obtained by averaging the simulation results over a period of 10 seconds (note that the first 120 s of simulation are disregarded from the average to allow the flow to fully developed).

The variations of HTC, Delta P and Delta T between inlet and outlet with different side tube distance to wall for chess pattern and uniform pattern are shown in Fig. 19 to Fig. 24. The HTC increases with the coil numbers due to enhanced mixing, while the pressure drop increases. The fluid Delta T increases with the number of coils, as a consequence of the increasing HTC.

With regards to the tubes geometrical arrangement, a higher heat transfer coefficient is obtained for the uniform tube arrangement configuration (Fig. 22) when compared to the chess configuration (Fig. 19)

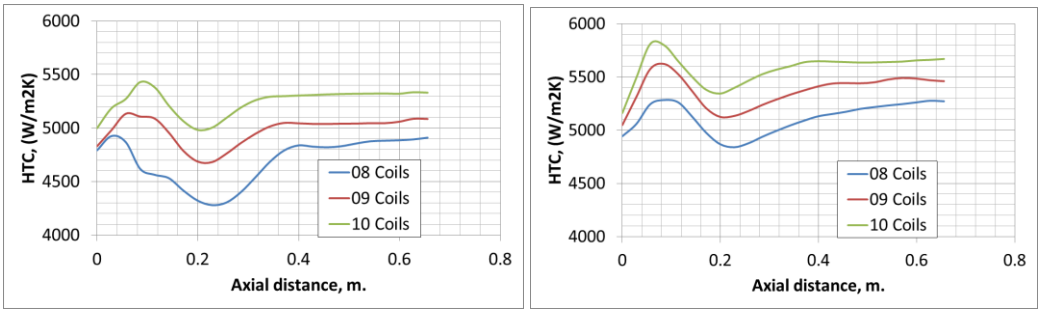

(a) (b)

Fig. 19 HTC comparison between different side tubes distance to wall for chess pattern, (a) Pitch/4; (b) Pitch/2

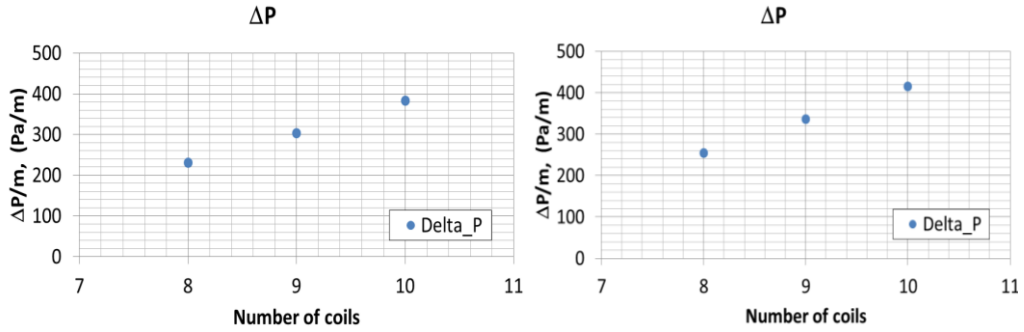

(a) (b)

Fig. 20 Delta P comparison between different side tubes distance to wall for chess pattern, (a) Pitch/4; (b) Pitch/2

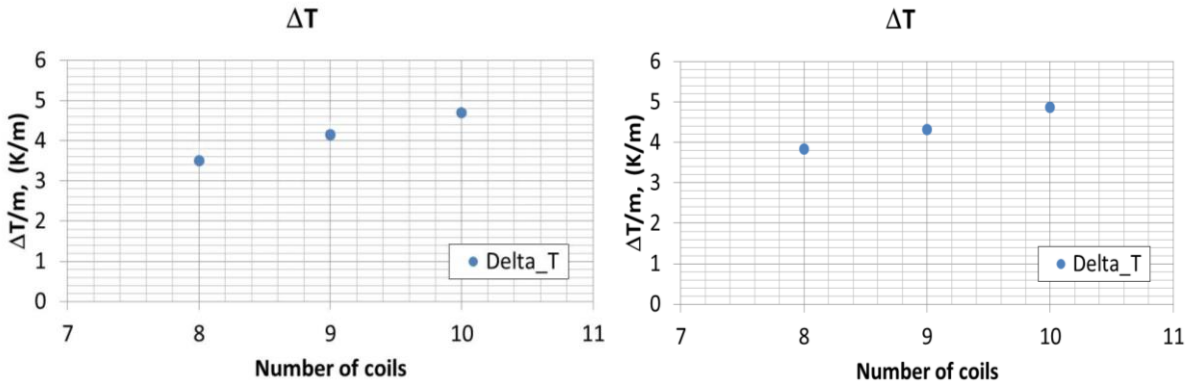

(a) (b)

Fig. 21 Delta T comparison between different side tubes distance to wall for chess pattern, (a) Pitch/4; (b) Pitch/2

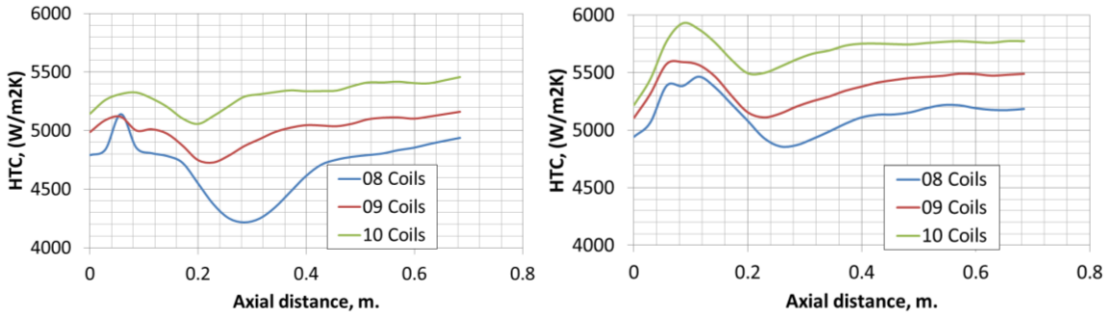

(a) (b)

Fig. 22 HTC comparison between different side tubes distance to wall for uniform pattern, (a) Pitch/4; (b) Pitch/2

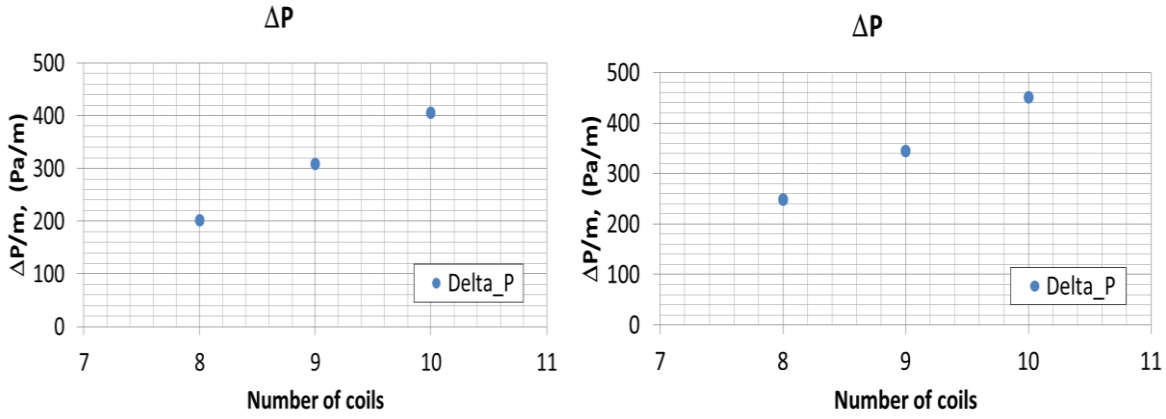

(a) (b)

Fig. 23 Delta P comparison between different side tubes distance to wall for uniform pattern, (a) Pitch/4; (b) Pitch/2

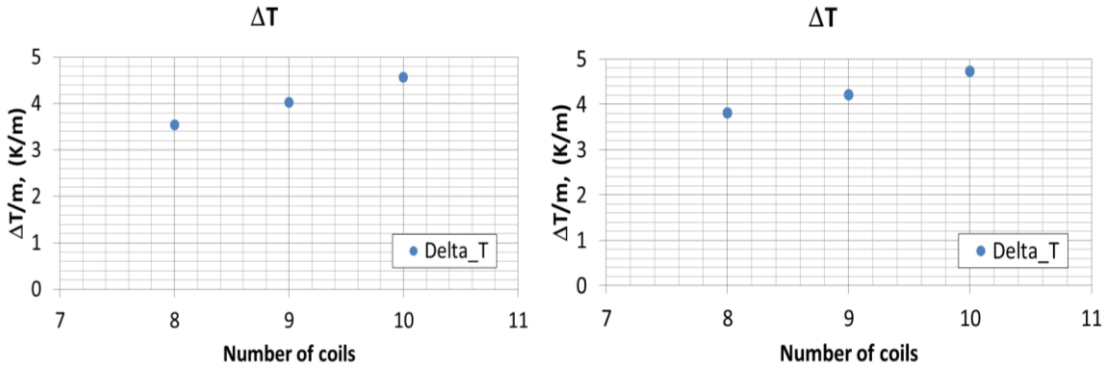

(a) (b)

Fig. 24 Delta T comparison between different side tubes distance to wall for uniform pattern, (a) Pitch/4; (b) Pitch/2

From the side tube distance point, Pitch/4 condition leads to a lower pressure drop, at the same time yielding a lower HTC. In order to evaluate the HX performance, we introduce the ratio θ, defined as:

$$\theta = \frac{h}{\Delta P} \tag{7}$$

The above ratio has the meaning of HTC variation per unit pressure drop. Higher ratio indicates better HX performance, e.g. a more optimal balance between HTC and pressure drops. For the pitch/2 condition, the ratio is about 16.18, while it is about 16.64 for the pitch/4 condition. Therefore, the tube arrangement type with pitch/4 condition is selected for the final HX design.

Based on the obtained results, the 9 coils option with about pitch/4 side tube distance is selected for the finalized DHR system design.

2.3.3 Intermediate loop and cooling tower sensitivity study

The intermediate loop and cooling tower loop play also an important role in determining the DHR heat transfer characteristic. Parametric studies are presented in this section. The analysis matrix is presented in Table 4.

Table 4 Analysis Matrix

Parameters	Value
Cooling tower height (m)	20, 25, 30, 35,40
Cooling tower inlet air temperature (K)	283.15, 288.15, 293.15, 298.15, 303.15, 308.15, 313.15, 323.15
Intermediate loop height difference (m)[#]	5.24, 10.24, 15.24, 17.74, 20.24, 22.74, 25.24
Intermediate loop pipe diameter (m)	0.1, 0.2, 0.3, 0.4, 0.5

Note: Height difference between the helical coil HX outlet and the air cooling HX inlet.

The results of the sensitivity study for the DHR intermediate loop and cooling tower are reported in Fig. 25 to Fig. 29. Figure 25 shows the heat removal capability of the DHR system for different cooling tower heights. As expected, the DHRS heat removal capability increases with increasing cooling tower height. However, significant increase of the heat removal performance is observed for cooling tower heights below 30 m. Increasing the tower height above 30 m yields only a moderate increase of the DHRS heat removal capacity. Given the cost of construction, a 30 m high cooling tower is deemed optimal. The cooling tower air mass flow rate is shown in Figure 26; it increases with tower height due to the increased buoyancy driving force. The DHR heat removal capacity for different atmosphere air temperature is presented in Figure 27. As expected, a certain variability exists in the DHRS performance depending on the atmosphere temperature. An air temperature of 288.15 K is used for further calculations. The results can be easily scaled to different atmosphere temperatures using the relationship between heat transfer, efficiency and temperature difference

between primary and secondary fluids. Figure 28 and Figure 29 show how the DHR heat removal characteristics are affected by the intermediate loop height difference and the intermediate loop pipe diameter. As expected, the mass flow rates in the intermediate loop increase with the height difference and the pipe diameter.

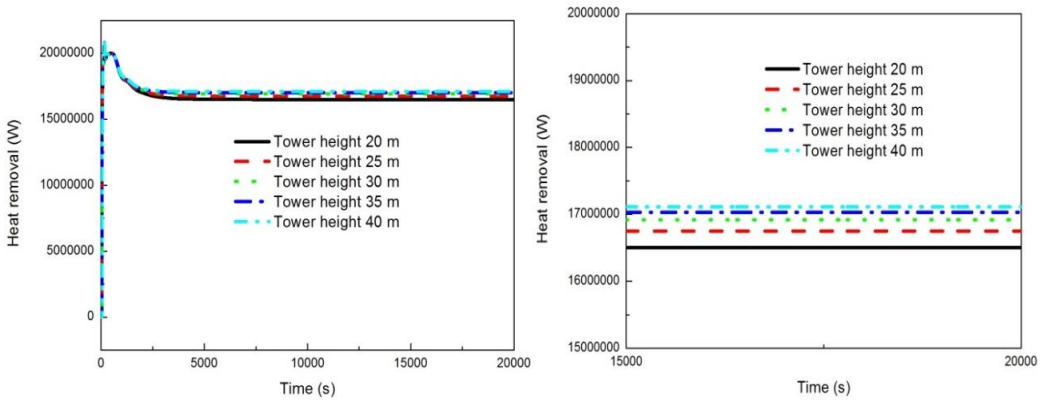

Fig. 25 Decay Heat Removal of Each DHRS Loop as a Function of Cooling tower height

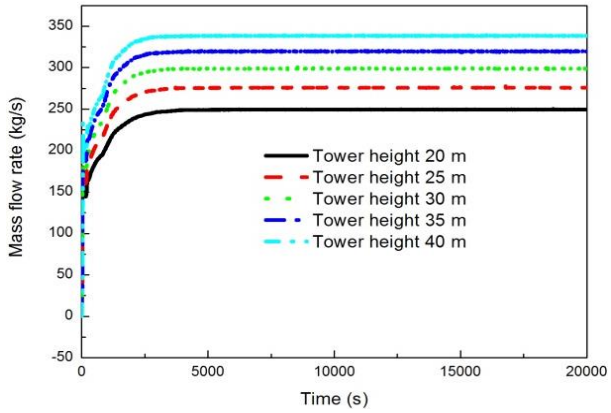

Fig. 26 Cooling tower air mass flow rate as a Function of Cooling tower height

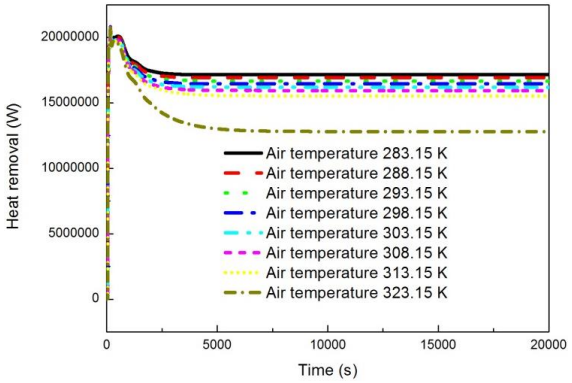

Fig. 27 Decay Heat Removal of Each DHRS Loop as a Function of atmosphere temperature

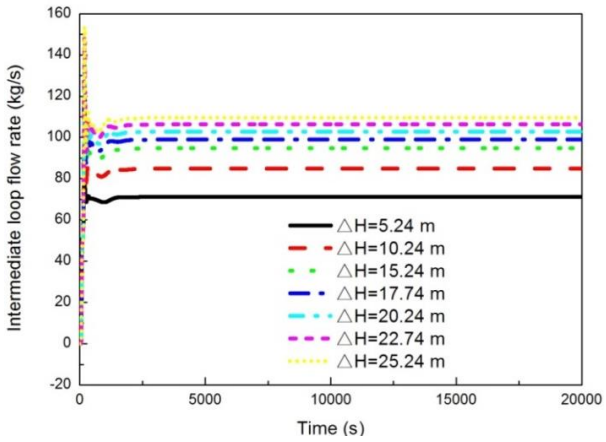

Fig. 28 Intermediate loop mass flow rate as a Function of intermediate loop height difference

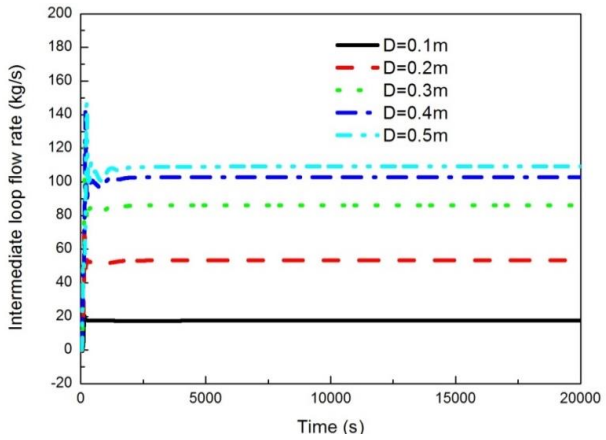

Fig. 29 Intermediate loop mass flow rate as a Function of intermediate pipe diameter

The sensitivity studies have shown that the DHRS is able to remove heat from the primary loop of the I^{2}S-LWR reactor at the desired rate. In the next section the performance of the DHRS is investigated in the event of a SBO accident, and the capability of indefinite heat removal is demonstrated.

3. I^{2}S-LWR Modeling

The I^{2}S-LWR primary loop has been modeled using the RELAP5 best-estimate thermal-hydraulic code. A RELAP5 nodalization of the I^{2}S-LWR RPV has been developed, consisting of four identical sections, each including a reactor coolant pump component, a PCHE component and a downcomer section. The reactor coolant pumps are located between the pressurizer (at the top of the RPV) and the PCHE.

A diagram of the RELAP5 nodalization for the I^2S-LWR primary loop, including the four DHRS trains is presented in Fig. 30. The reactor downcomer is divided into four parts and each part contains a PCHE component and a corresponding DHRS train. In the RELAP5 model, the reactor vessel, core, pressurizer, reactor coolant pumps, PCHE and DHRS are modeled in detail. The lower plenum and upper plenum are modeled using pipes. The downcomer region is divided into four branches and the four DHR systems are connected with the reactor downcomer using junctions. The heat loss from the vessel and reactor internals is ignored due to the very limited influence on the transient simulation. The reactor core is simulated with bypass pipe, hot pipe and average pipe and it is divided into 10 nodes in the axial direction. The heat structure model is employed to simulate the heat transfer in the core. The primary heat exchanger is modeled using a pipe with 20 nodes and the heat exchange is modeled with the heat structures. The pressurizer is divided into the lower part and upper part. The holes with great resistance coefficient are featured as the surge lines in the loop-type PWR and simulated with the junction. The pump sealing structure is ignored during the system longtime safety analysis [28]. The core heat power is set as a fixed value in the normal operation with an actual axis distribution, while the ANS-97 decay heat curve is employed to model the heat power variation in the reactor shutdown process [30]. The material properties, including U_3Si_2, Advanced steels APMT, carbon steel and stainless steel, are input as the general tables. Additional auxiliary systems needed for the simulations are modeled using Time Dependent Volumes (TMDPVOLs) and Time Dependent Junctions (TMDPJUNs), such as the primary heat exchanger secondary inlet mass flow rate, pressure, temperature and the containment environment.

4. Results and Analysis

4.1 Steady State Calculation

A steady state calculation is first performed using the I^2S-LWR RELAP5 nodalization, and the obtained results have been compared with the design parameters, as reported in Table 5. The nominal reactor thermal power is set to 2850 MWt, and the equivalent PCHE secondary side flow rate is equal to 3128.25 kg/s per PCHE, based on an optimization study on the efficiency of the I^2S-LWR thermodynamic cycle [4].

Table 5 Steady state results and comparison with designed value

Parameters	Designed value	Calculated value	Errors
Core inlet temperature (K)	571.15	567.60	0.45%
Core outlet temperature (K)	602.15	600.49	0.75%
Reactor pressure (MPa)	15.5	15.49	0.006%
Core flow rate (kg/s)	15467	15467.1	0.0%
Pressurizer water level (m)	3.24	3.24	0.0%

As shown in table 5, the RELAP5 steady state results are in good agreement with the design parameters. The errors of important thermal hydraulic parameter results between calculated values and design values are within 2.0%. In the next section, the Relap5 nodalization is used to simulate a SBO transient.

4.2 SBO Transient Study

Starting from steady-state conditions at nominal operation, a SBO event is assumed to occur at 0 s. Consequent to the loss of power, the primary circuit pumps begin to coast down. The PCHE secondary feed water is assumed to decrease to 0 kg/s within 200 s. In order to be conservative, no credit is taken for the PCHE heat removal after the first 250 s of transient. Also, no credit is taken for the availability of any diesel generator. The DHRS valves, located in the intermediate loop, open upon receipt of the reactor shutdown signal, assuming 5 s delay of signal transfer. The accident logic for the SBO event is listed in Table 6. The reactor decay heat curve [28] is shown in Figure 31. In the following sections, the evolution of the SBO event is investigated assuming four DHRs, three DHRs and two DHRs are in operation, respectively.

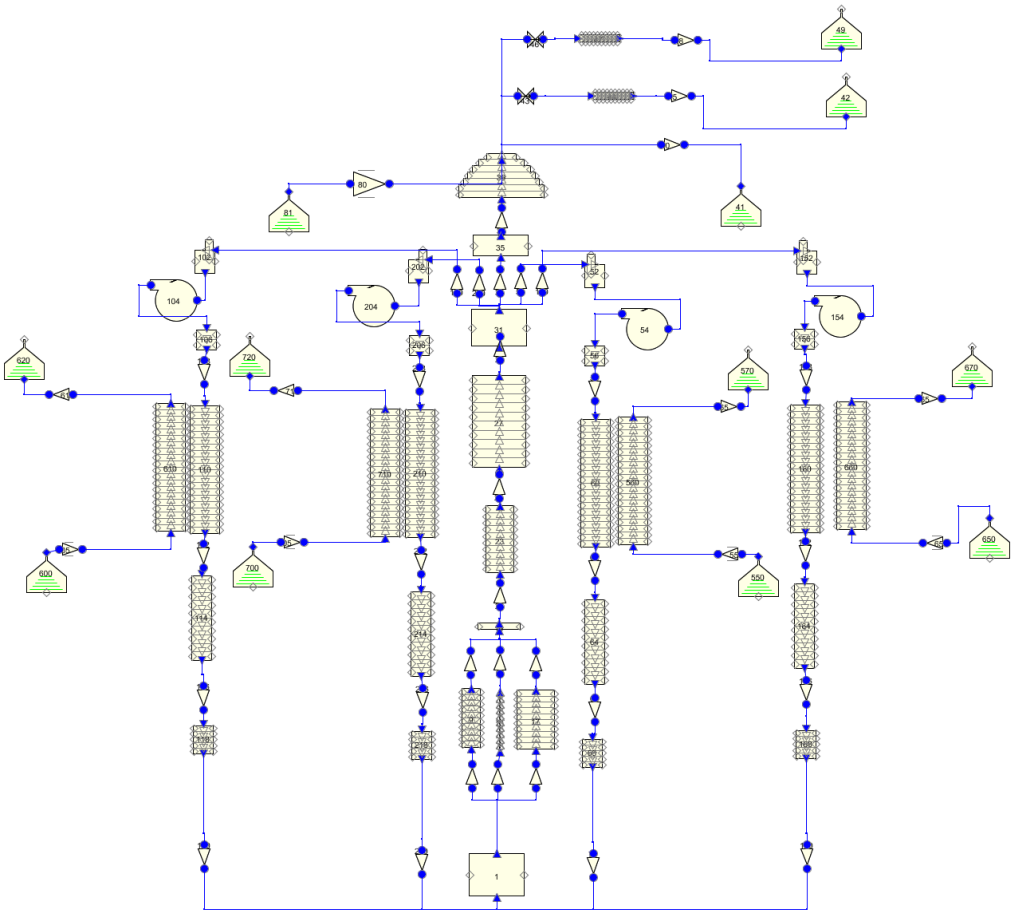

(a) I^{2}S-LWR primary loop

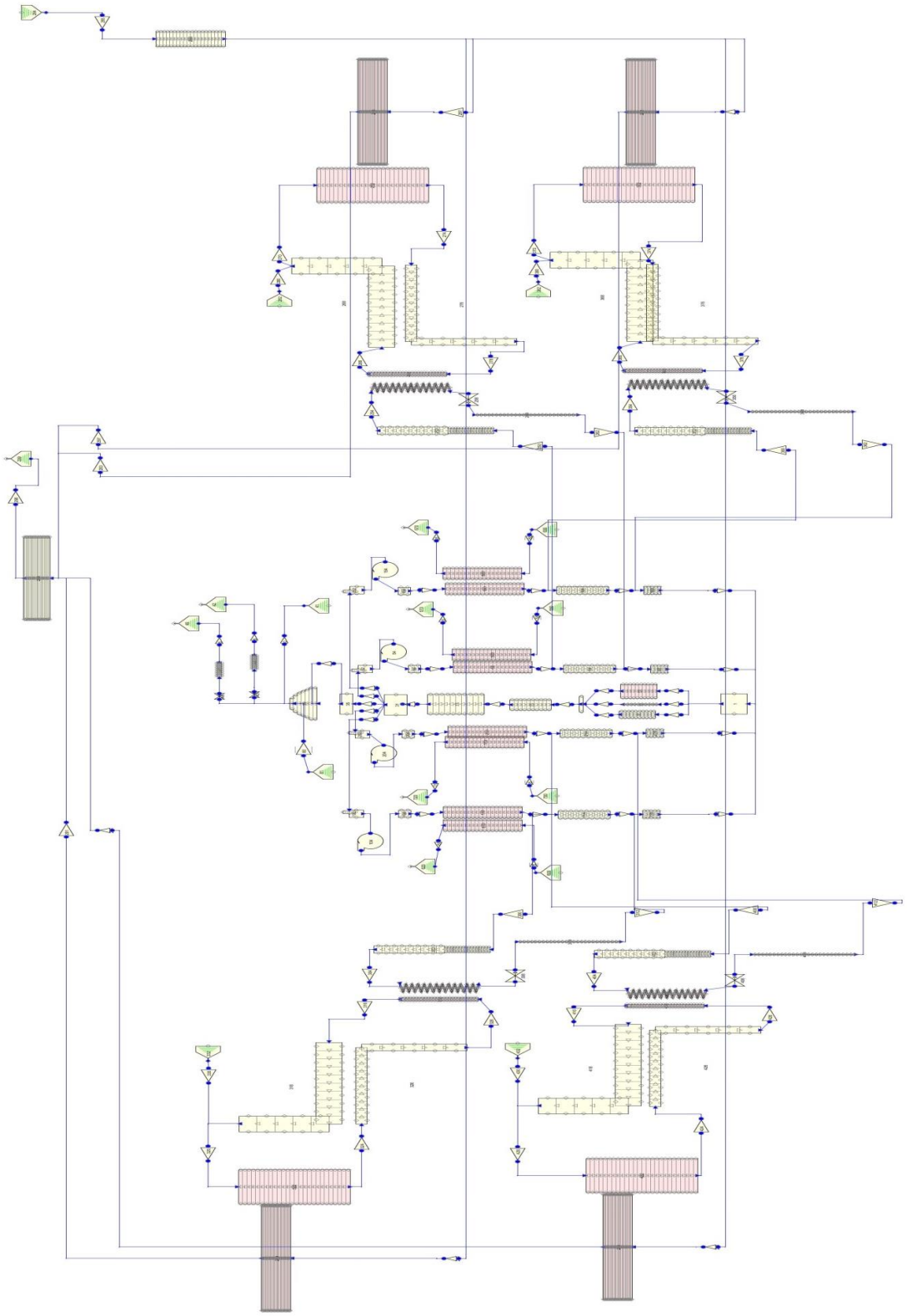

(b) The primary loop and DHRs

Fig. 30 I^{2}S-LWR and DHRs Relap5 Nodalization

Table 6 Event sequence of SBO

Event	Time (s)
SBO occurs	0.0
Reactor shutdown trip	0.0
Secondary side flow rate trip	0.0 (200 s decrease to 0)
Pump run out trip	0.0 (Coast down time 250 s)
DHR valve open trip	5.0

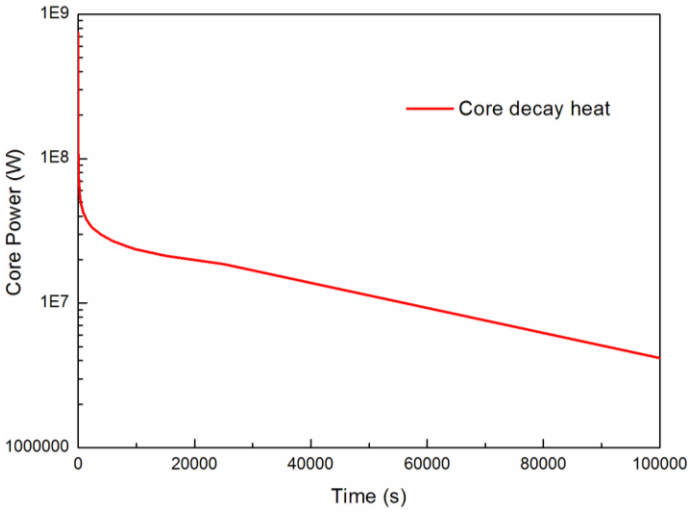

Fig. 31 I^{2}S-LWR reactor core decay heat curve

4.2.1 Four DHR systems in operation

In this section, the SBO scenario is studied assuming four DHRs in operation. Relevant time traces are shown in Fig. 32 to Fig. 36.

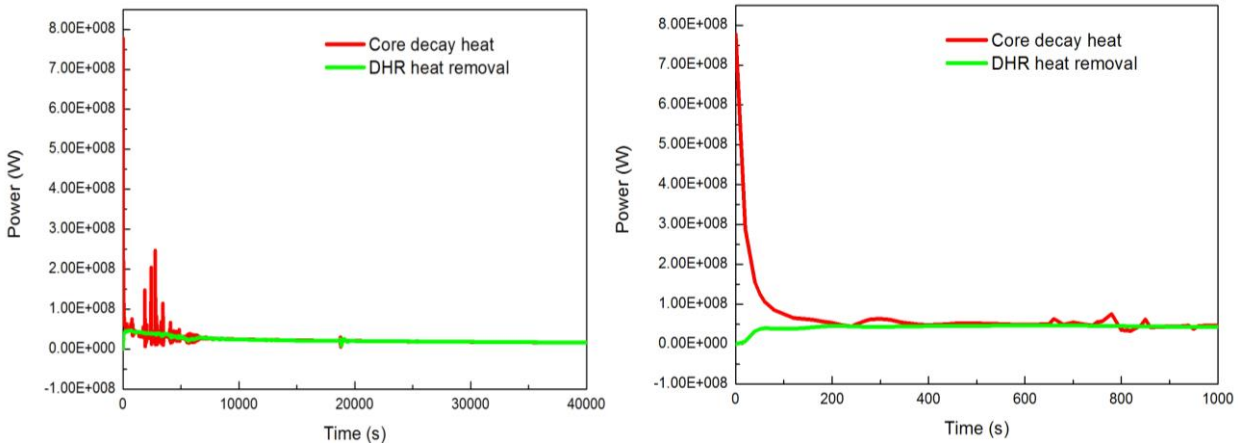

Fig. 32 Variations of decay heat and DHRs heat removal vs time

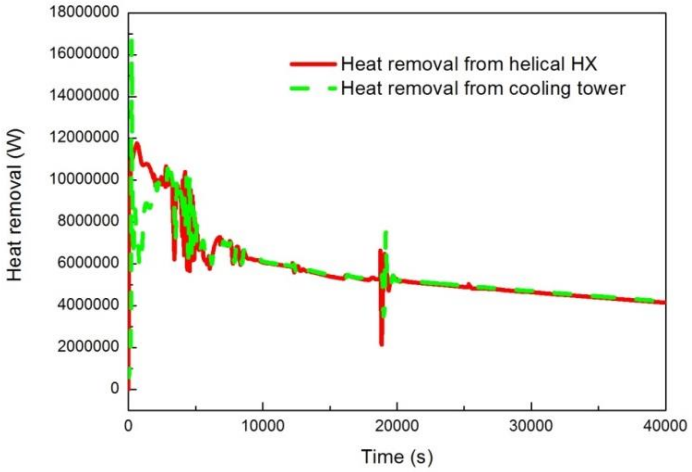

Fig. 33 Variations of primary loop HX and intermediate loop heat removal vs time

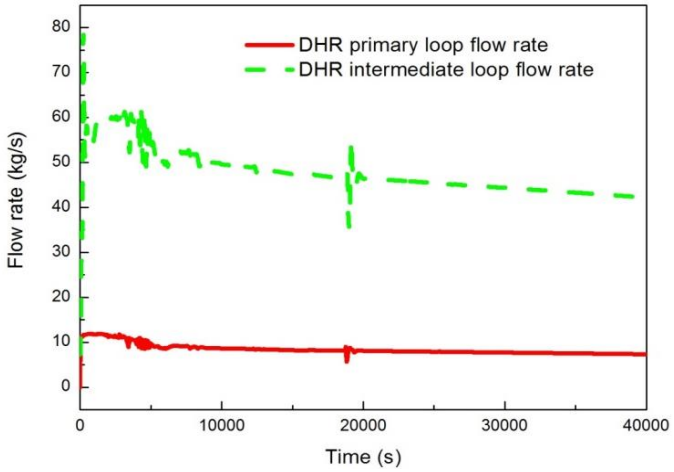

Fig. 34 Variations of primary loop HX and intermediate loop flow rate vs time

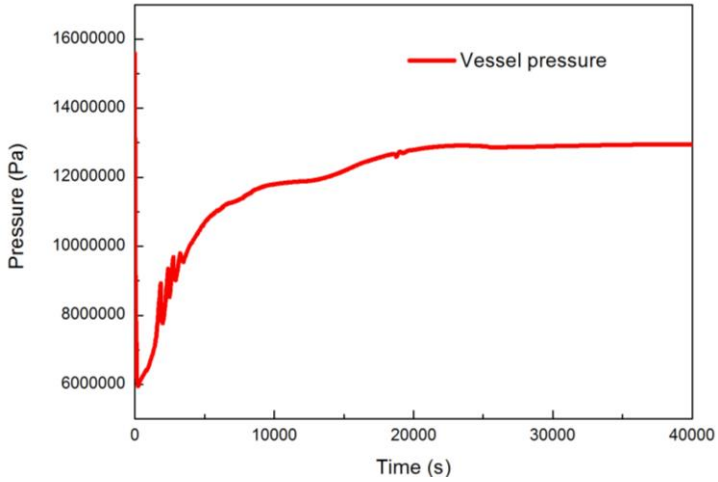

Fig. 35 Variations of primary pressure vs time

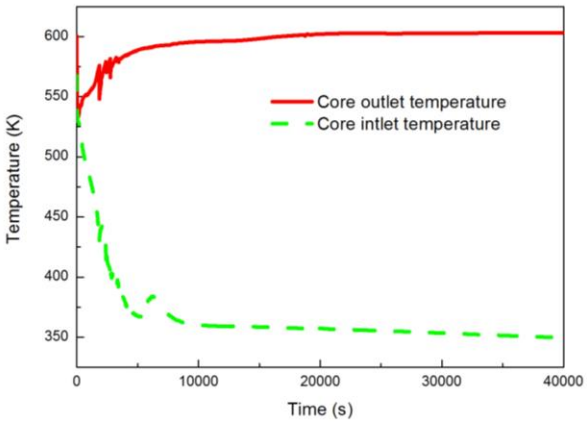

Fig. 36 Variations of core inlet and outlet temperatures vs time

As shown in Fig. 32, the DHRs heat removal matches the decay heat at about 200 s, successfully providing indefinite decay heat removal in case of an SBO scenario. Heat removal from intermediate and cooling tower loop are presented in Fig. 33, while Fig. 34 reports the mass flow rate in the primary and secondary loop of one of the DHR trains. The I^2S-LWR reactor primary loop variables, including pressure and core temperature, are shown in Fig. 35 and Fig 36. The RPV pressure stabilizes at about 12.5 MPa and the core outlet temperature remains around 600 K, without the need of any other auxiliary active system.

4.2.2 Three DHR systems in operation

Also in case only three DHR trains are in operation, indefinite heat removal capabilities are successfully demonstrated, as shown in Fig. 37. However, a longer time interval (around 2000 s) is needed to establish equilibrium between decay heat and DHR heat removal rate, The RPV pressure stabilizes around 14.5 MPa (see Fig, 38) while the core temperature remains below 620 K (see Fig. 39). Nevertheless, also in case of only three DHR trains in operation, during a SBO event the reactor can be maintained in safe conditions for an indefinite period of time, without the need of any additional system.

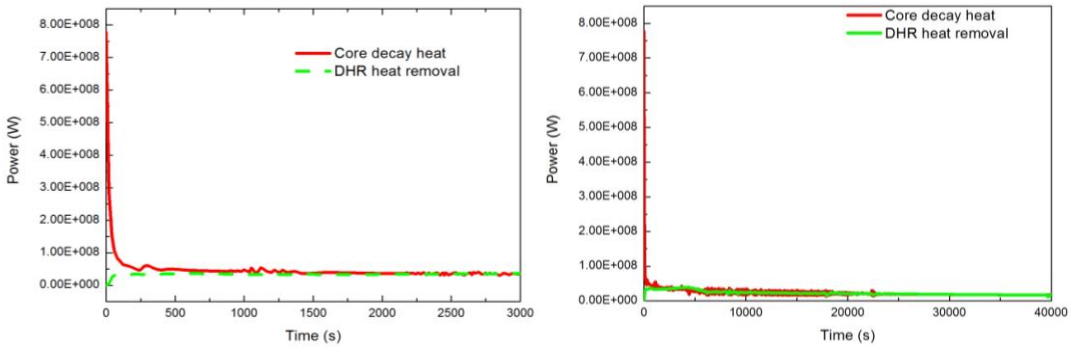

Fig. 37 Variations of decay heat and DHRs heat removal vs time

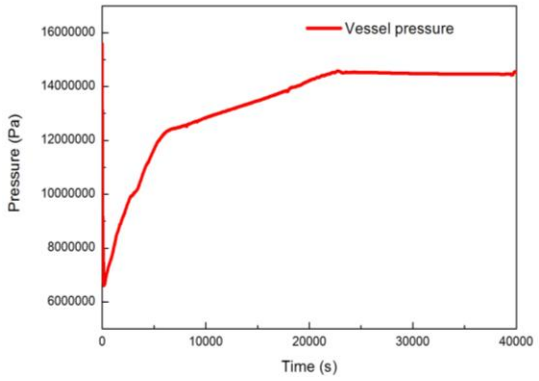

Fig. 38 Variations of primary pressure vs time

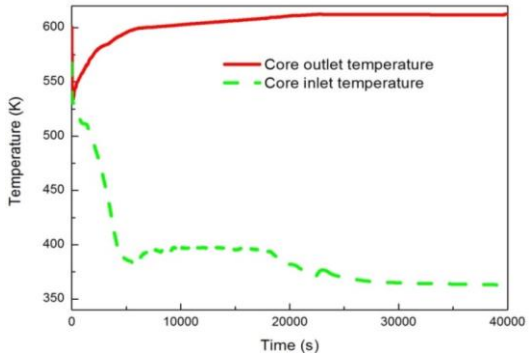

Fig. 39 Variations of core inlet and outlet temperatures vs time

4.2.3 Two DHR systems in operation

Finally, the evolution of a SBO event in case two DHRs are in operation is analyzed. As shown in Fig. 40 to Fig. 42, in this case the DHRs heat removal rate does not match the core decay heat until nearly 5000 s into the transient. During this time interval, unacceptable levels for the RPV pressure and core temperature are established. As by design, it is therefore demonstrated that a minimum of three operating DHR trains are required.

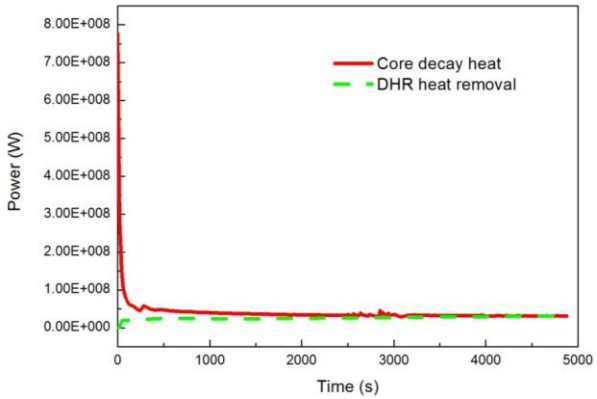

Fig. 40 Variations of decay heat and DHRs heat removal vs time

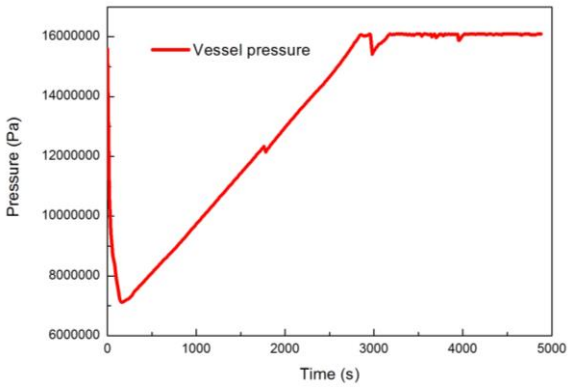

Fig. 41 Variations of primary pressure vs time

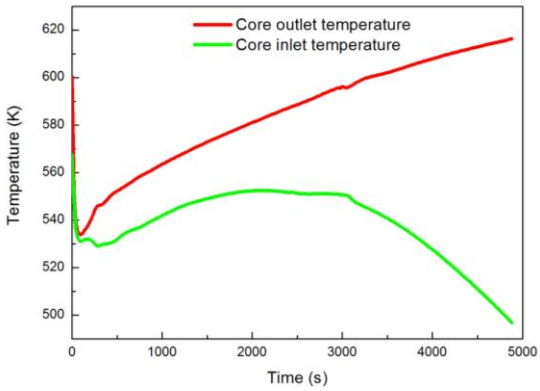

Fig. 42 Variations of core inlet and outlet temperatures vs time

5. Conclusions

In this paper, a passive DHRS, consisting of a primary HX located in the RPV, a secondary HX located in a dry cooling tower, a fail-open valve, and the required piping between these components, is proposed for the I^2S-LWR design. The geometry of the DHRS components is optimized using engineering consideration, combined with one dimensional and three dimensional computational methods. The performance of the optimized DHRS design is then investigated against a SBO event using the best-estimate thermal-hydraulic code RELAP5. Based on the comprehensive investigations, the following conclusions could be drawn.

The basic geometry design of DHRS, including the helical coil HX, cooling tower and the configuration arrangement, is confirmed. The DHRS RELAP5 model is built and the heat removal analysis is performed. The height of 8.0 m allows a heat removal capability of about 17.5 MW per DHRS train. Considering the reactor core power level and the redundant design concept, four DHR systems are determined for the I^2S-LWR design.

Based on the detailed three-dimensional study for the helical coil HX, considering the balance between the heat transfer and flow pressure drop, the 9 coils option with about pitch/4 side tube distance is selected for the finalized DHR system design. For the cooling tower part, the pipe horizontal configuration with rectangular arrangements is adopted and given the cost of construction, a 30 m high cooling tower is deemed optimal.

The whole I^2S-LWR primary loop RELAP5 model is established and the DHRS is integrated with the primary loop. The primary loop system responses and the DHRS performances are studied in case of SBO accident scenario. The results show that, as by design, three out of four DHRS trains are sufficient (and required) to successfully remove the core residual heat in the event of a SBO transient. It has also been demonstrated that indefinite cooling, using atmosphere as the ultimate heat sink, can be achieved successfully.

Acknowledgments

This research has been supported by the Chinese Scholarship Council and by the US DOE Office of Nuclear Energy's Nuclear Energy University Programs (NEUP).

References

1. B. Petrovic, 2014. The Integral Inherently Safe Light Water Reactor, Nuclear Engineering International, 59(716): 26-29.
2. M. D. Carelli, L. E. Conway, L. Oriani, B. Petrovic, C. V. Lombardi, M. E. Ricotti, A. C. O. Barroso, J. M. Collado, L. Cinotti, N. E. Todreas, D. Grgic, M. M. Moraes, R. D. Boroughs, H. Ninokata, D. T. Ingersoll, F. Oriolo, 2004. The Design and Safety Features of the IRIS Reactor, Nuclear Engineering and Design, 230: 151-167.
3. M. Smith, R. Wright, 2012. Westinghouse Small Modular Reactor Passive Safety System Response to Postulated Events, ICAPP'12, Chicago, June 24-28, USA.
4. M. Memmott, A. Manera, 2015. The Use of a Flashing Drum to Generate Steam in the Integral, Inherently Safe (I^2S) Light Water Reactor, Nuclear Technology, 191(3): 199-212.
5. I^2S-LWR Project Team, 2013. Integral Inherently Safe Light Water Reactor (I^2S-LWR), Quarterly Progress Report (2013_Q3 April-June 2013).
6. J. C. DeVine, 1996. Conceptual benefits of passive nuclear power plants and their effect on component design, Nucl. Eng. Des. 165: 299-305.
7. M. Wang, W. Tian, S. Qiu, G. Su, Y. Zhang, 2013. An evaluation of designed passive Core Makeup Tank (CMT) for Chinapressurized reactor (CPR1000), Annals of Nuclear Energy. 56: 81-86.

8. M. Wang, H. Zhao, Y. Zhang, G. H. Su, W. Tian, S. Qiu, 2012. Research on the Designed Emergency Passive Residual Heat Removal System During the Station Blackout Scenario for CPR1000 [J]. Annals of Nuclear Energy, 45: 86-93.
9. P. E. Juhn, J. Kupitz, J. Cleveland, B. Cho, R. B. Lyon, 2000. IAEA activities on passive safety systems and overview of international development. Nucl. Eng. Des., 201(1-2): 41-59.
10. T. L. Schulz, 2006. Westinghouse AP1000 advanced passive plant, Nucl. Eng. Des. 236(14-16: 1547-1557.
11. A. Morozov, A. Soshkina, 2008. Passive Core Cooling Systems for Next Generation NPPs: Characteristics and State of the Art. IYNC 2008, September 20-26, Interlaken, Switzerland.
12. S. Agamy, A.M. Metwally, M. Al-Ramady, S.M. Elaraby, 2010. A RELAP5 model for the thermal-hydraulic analysis of a typical pressurized water reactor, Therm. Sci. 14(1): 79-88.
13. R. Ferri, A. Achilli, G. Cattadori, F. Bianchi, P. Meloni, 2005. Design, experiments and RELAP code calculations for the PERSEO facility, Nucl. Eng. Des. 235: 1201-1214.
14. IAEA, 1991. Safety related terms for advanced nuclear power plants. IAEA-TECDOC- 626.
15. M. Wang, A. Manera, M. J. Memmott, S. Qiu, 2018. Preliminary Design of the I^2S-LWR Containment System, Annals of Nuclear Energy, (DOI: https://doi.org/10.1016/j.anucene.2018.03.014)
16. A. Manera, M. Memmott, 2014. Design and trade-off studies of the passive heat decay removal system (DHRS) of the Integral Inherently Safe LWR (I^2S-LWR), Proc. 10th International Conference on Nuclear Option in Countries with Small and Medium Electricity Grid, June 2014, Zadar, Croatia.
17. L. Cinotti, M. Bruzzone, N. Meda, G. Corsini, C.V. Lombardi, M. Ricotti, L. E. Conway, 2002. Steam Generator of the International Reactor Innovative and Secure, Proc. 10th ICONE, April 14-18, Arlington, USA.
18. D. Bünemann, M. Kolb, H. Henssen, E. Müller, W. Rossbach, 1972. THE CORE DESIGN OF THE REACTOR FOR THE NUCLEAR SHIP "OTTO HAHN, Advances in Nuclear Science & technology, 6:1-44.
19. J.N. Reyes, 2012. NuScale Plant Safety in Response to Extreme Events, Nuclear Technology. 178, pp. 153-163.
20. B. J. Webb, 2011. Design Aspects of Once-through Helical Coil Steam Generators, Proceedings of the ASME 2011 Small Modular Reactors Symposium, SMR2011-6630, Washington, DC, USA.
21. K. K. McKelvey and M. Brooke, 1959. The Industrial Cooling Tower, Elsevier Publishing Company.
22. D. Busch, R. Harte, W. B. Kraetzig, U. Montag, 2002. New natural draft cooling tower of 200 m of height, Engineering Structures 24: 1509-1521.
23. F. K. Moore, 1976. Dry Cooling Towers, Adv. Heat Transfer, 12: 1-75.
24. J. R. Singham, 1990. Natural Draft Towers," Section 3.12.3, Hemisphere Handbook of Heat Exchanger Design, Hemisphere Publishing Corporation, New York, USA.

25. G. Caruso, M. Fatone, A. Naviglio, 2007. An experimental study on natural draft-dry cooling tower as part of the passive system for the residual decay heat removal," Proceedings of ICAPP 2007, May 13-18, Nice, France.
26. A. D. Nevo, D. Rozzia, N. Forgione, 2013. MODELING THE HEAT TRANSFER OF HELICAL COIL TUBES STEAM GENERATOR IN SMR BY RELAP5 CODE AND VALIDATION, NURETH-15, May 12-15, Pisa, Italy.
27. RELAP5/MOD3.3, 2001. Code Manual Volume 1: Code Structure, System Models, and Solution Methods NUREG/CR-5535.
28. RELAP5/MOD3.3, 2001. Code Manual Volume V: User's Guidelines NUREG/CR-5535.
29. M. J. Memmott, A. Manera, J. Boyack, S. Pacheco, M. Wang, B. Petrovic, 2017. The primary reactor coolant system concept of the integral, inherently safe light water reactor. Annals of Nuclear Energy, 100: 53-67.
30. N. E. Todreas and M. S. Kazimi, 1990. Nuclear Systems I, Thermal Hydraulic Fundamentals, Hemisphere Publishing Corporation, ISBN 0-89116-935-0 (V. 1).